Design and Performance of a High-T_c Superconductor Coplanar Waveguide Filter

Wilbert Chew, A. Landis Riley, *Member*, *IEEE*, Daniel L. Rascoe, *Member*, *IEEE*, Brian D. Hunt, Marc C. Foote, Thomas W. Cooley, and Louis J. Bajuk

***Abstract*—Coplanar waveguide is a convenient structure for microwave circuits using high-critical-temperature superconductor thin films. The design of a coplanar waveguide low-pass filter made of $YBa_2Cu_3O_{7-\delta}$ (YBCO) on an $LaAlO_3$ substrate is described. Measurements were incorporated into simple models for microwave CAD analysis to develop a final design. The patterned and packaged coplanar waveguide low-pass filter of YBCO, with dimensions suited for integrated circuits, exhibited measured insertion losses when cooled in liquid nitrogen superior to those of a similarly cooled thin-film copper filter throughout the 0 to 9.5 GHz passband. Coplanar waveguide models for use with thin-film normal metal (with thickness either greater or less than the skin depth) and YBCO are discussed and used to compare the losses of the measured YBCO and copper circuits.**

I. Introduction

LOW-LOSS thin-film microwave circuits are a direct and immediate application of high-temperature (high T_c) superconductors, which can be fabricated as high-quality aligned films on suitable substrates. Coplanar waveguide (CPW) [1] is a particularly convenient thin-film structure, requiring the coating of only one side of a substrate with superconductor and thereby allowing the other side to be thermally anchored during deposition and *in situ* annealing of the superconductor. CPW resonators made of $YBa_2Cu_3O_{7-\delta}$ (YBCO) have shown losses superior to those of copper at 77 K [2], [3]. We have made CPW low-pass microwave filters of YBCO on $LaAlO_3$ substrates which exhibit losses lower than those of comparable copper or silver filters at 77 K [4].

The filter structure consisted of sections of CPW transmission lines having dimensions suitable for integrated circuits. The filter design is shown in Fig. 1. The filter included tapered microstrip-to-CPW transitions at the input and output, 50 Ω CPW transmission lines near the input and output, and nine alternating low- and high-impedance CPW transmission line sections. The substrate was 10 mm×10 mm×0.5 mm $LaAlO_3$. The line width of the central conductor in the narrow high-impedance sections was 5–10 μm, a practical line width for integrated circuit applications. The spacing of the coplanar grounds (center line width plus two gap widths) was 250 μm, a spacing compatible with standard wafer probes. The widths of the center conductors in the low-impedance and 50 Ω sections were 200 μm and 50 μm, respectively. This low-pass filter was designed for a 0 to 9.5 GHz passband. Further structure and fabrication details are given in [4]. The narrow line widths and large area used for the filter, which could be typical in integrated circuit applications, provided a stringent test of the usefulness and practicality of currently available YBCO. Similar segments of transmission lines made of thin-film superconductors can be used to make a broad range of microwave circuits, as well as low-loss and low-dispersion interconnections for monolithic microwave integrated circuits (MMIC's) or high-speed digital integrated circuits. The complete filter gives a true idea of the advantages and difficulties of replacing thin-film metal with high-temperature superconductor in a fully patterned and packaged practical circuit. While this circuit does not provide material parameters as directly as simpler test structures, approximate conductivity or loss values can be found by fitting measured data with calculated filter responses using models for the superconductor and normal-metal coplanar waveguide lines.

II. Design

When the design began, various values for the permittivity of $LaAlO_3$ had been published [5]–[7]. Models for CPW discontinuities and losses were lacking in the available commercial microwave circuit computer-aided design (CAD) software. A set of CPW test structures (Fig. 2) having the 250 μm ground plane spacing and 10, 50, and 200 μm center line widths intended for the filter designs was fabricated in 1-μm-thick silver film on $LaAlO_3$. These test structures had the step discontinuities between the different line widths to be used and different lengths of transmission line sections. The S parameters of these test structures were measured using a standard commercial

Manuscript received October 15, 1990. This work was supported by the Office of Aeronautics and Exploration Technology of the National Aeronautics and Space Administration, by the Defense Advanced Research Projects Agency, and by the Innovative Science and Technology Office of the Strategic Defense Initiative Organization.

The authors are with the Center for Space Microelectronics Technology, Jet Propulsion Laboratory, California Institute of Technology, Pasadena, CA 91109.

IEEE Log Number 9101130.

0018-9480/91/0900-1455$01.00

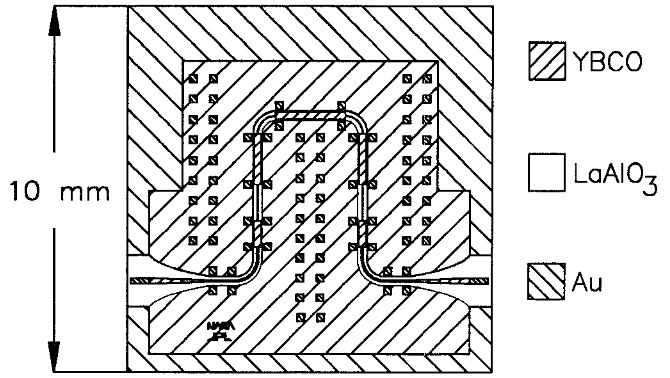

Fig. 1. Top surface of coplanar waveguide filter. Gold areas have YBCO underneath. Bond wires connect ground conductors at pads near steps.

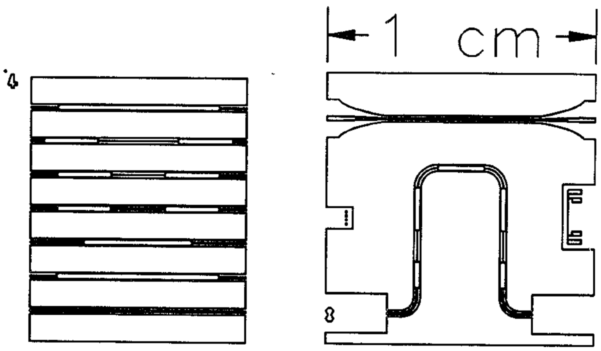

Fig. 2. CPW test structures for normal metal.

wafer probe and a microwave network analyzer, with "full two-port" calibration using the impedance standards on a Cascade Microtech impedance standard substrate [8].

The test structures were modeled, using the commercial microwave CAD software EEsof Touchstone, as cascaded lengths of transmission line. A step discontinuity was simply modeled as a variable extra length of the wider line (for the fringing capacitance of the step) with an equal lessened length of the narrower line at each kind of step. Another variable was the effective permittivity. Using the software to optimize the fit of the measured data to the model by adjusting the variables gave approximate extra effective lengths of 17 μm for the 200 μm lines at junctions with 50 μm lines and lengths of 18 μm for the 200 μm lines at junctions with 10 μm lines, together with an effective relative permittivity of 12.8 for the CPW lines (or a relative permittivity of approximately 25 for $LaAlO_3$.) The substrate was thick enough for the bottom surface metallization to have only a minor effect on the CPW characteristics [9]. Modal dispersion effects were expected to be small below 11 GHz [10] and were not included to simplify the modeling. More complex models could be used for the step junctions, but simpler models are more reliable when fitting limited data. The effective permittivity calculated for ideal CPW does not vary much with the line dimensions used, so a single value was used for modeling. The effective lengths and effective permittivity can be calculated directly from the resonance frequencies of such test structures [11], but modeling using optimization in the CAD software allowed a weighted average "best fit" using all the swept frequency data measured. A general transmission line element was used instead of a coplanar waveguide element in the Touchstone model to allow the use of different models for transmission line attenuation. Since the usual $f^{1/2}$ frequency dependence of the attenuation constant, α_n, for a normal-metal transmission line assumes shallow field penetration and becomes inapplicable at low frequencies, an empirical expression was substituted:

$$\alpha_n = \alpha_{n0}(f/f_0)^{1/2} + \alpha_{n1} \tag{1}$$

where f_0 is a reference frequency, and α_{n0} and α_{n1} are adjustable parameters. The α_n's for each line width are different, and were chosen to have the same ratios as predicted using formulas for shallow field penetration. Because the effect of attenuation in the narrow (10 μm wide) lines dominated the effects of attenuation in the wider lines, more exact values were not required for the design. Further analysis discussed later gives approximate results for all the lines in a consistent way.

After determining the step model and the permittivity, a CPW filter was designed, assuming no loss, by using Touchstone to optimize the design line lengths for the desired low-pass response. Both silver and YBCO versions were fabricated and mounted in test fixtures on copper blocks. (The YBCO filter went through essentially the same processing procedure as the final filters described later, except for the final bakeout and package welding.) Their S parameters were measured with the network analyzer. Thru-reflect-line calibration [12] fixtures on copper blocks were used to calibrate out the losses up to the input and output of the structure on the $LaAlO_3$ substrate. Direct immersion in liquid nitrogen would change the measured effective permittivity compared with measurement in vacuum; also, measured losses were higher in the liquid nitrogen. So, instead, only the copper blocks were immersed in the liquid nitrogen, with the filter surface above the liquid. A temperature sensor was mounted near the filter substrate to check that the fixture was at 77 K.

The silver film filter showed performance consistent with the model. The YBCO film filter was expected to show a frequency shift caused by kinetic inductance in the superconductor [13] but the magnitude of the effect varied among samples. A YBCO filter made from a film chosen for high dc critical current and high T_c showed an acceptable frequency shift, as well as a loss less than that of the silver filter. (A variation of less than 1 GHz as temperature varied from 70 to 80 K was needed for this application; this YBCO filter cutoff varied by about 0.5 GHz from 70 to 80 K.)

A circuit model for the YBCO filter consisted of sections of general transmission line like the circuit model for the silver filter, except for a different empirical loss model and a factor to model the effect of the increased

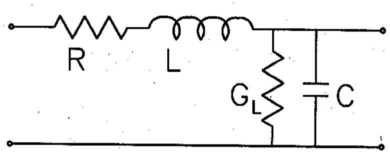

Fig. 3. Differential length (dz) of general transmission line model. R usually represents conductor losses and G_L usually represents dielectric losses.

inductance. The increased inductance affects the phase velocity, v, as well as the impedances of the transmission line sections. For a general transmission line (Fig. 3) with an inductance/length L, a capacitance/length C, and low losses (low series resistance/length R and low shunt conductance/length G_L), the characteristic impedance, Z, and the phase velocity, v, are [14]

$$Z = \sqrt{\frac{R + j\omega L}{G_L + j\omega C}} \approx \sqrt{L/C} \quad [\Omega] \tag{2}$$

$$v \approx 1/\sqrt{LC}. \tag{3}$$

Thus, the increased inductance was modeled as a factor which decreased the phase velocity and increased the characteristic impedance of each section of transmission line:

$$v \approx 1/\left(K\sqrt{L_e C}\right) \tag{4}$$

$$Z \approx K\sqrt{L_e/C} \quad [\Omega] \tag{5}$$

where

$$K^2 = L/L_e. \tag{6}$$

L is the total inductance/length, and L_e is the "external" inductance/length of the transmission line excluding contributions from within the conductor. (The effective permittivity of the general transmission line element was used to control the phase velocity on the transmission line in the CAD software.) Further analysis discussed later indicates that the increased inductance effect was concentrated in the narrow line sections, but the minor design change necessary to get the desired passband was made by assuming an average wave-slowing factor for the entire filter. The superconductor attenuation was assumed to increase with the square of the frequency:

$$\alpha_{sc} = \alpha_{sc0}(f/f_0)^2 \tag{7}$$

where α_{sc0} is an adjustable parameter and f_0 is the reference frequency. Approximate values of 1.03 for average K and values of 13, 18, and 44 dB/m for α_{sc0} for nominal 50-, 200-, and 10-μm-wide lines at a reference frequency $f_0 = 9$ GHz were found by optimizing the fit of the model to the measured S parameters for the YBCO filter. These values were then used to obtain the final filter design (Fig. 1) with the section lengths in Table I.

III. Results

The final filters, using *in situ* annealed films deposited by laser ablation, were patterned by argon ion milling, as described in [4]. No postannealing was done after patterning. The patterned line widths were narrowed by approximately 4 μm from the design widths listed above, with the line narrowed more at the top surface of the YBCO film than at the YBCO–substrate interface. The average YBCO film thickness was 0.5 μm. Critical current and T_c measurements were made on the patterned filters to select those suitable for assembly. (Good filters had zero-resistance $T_c > 83$ K and critical current density $J_c > 4 \times 10^5$ A/cm^2 at 77 K; the best had $T_c = 87.8$ K and $J_c = 8.1 \times 10^5$ A/cm^2.) Wire bonds made by thermosonic bonding of 0.0007 in. gold wire on gold pads deposited on the YBCO passed wire bond pull tests at 2 grams. The filters were assembled and sealed in Kovar packages by welding in vacuum. The packaged filter before welding on the lid is shown in Fig. 4.

TABLE I
Section Dimensions of Filter Design (Ground Plane Separation of 0.250 mm)

Section	Length (mm)	Width (mm)	Characteristic Impedance (Ω)
1,9	0.721	0.200	23
2,8	0.997	0.010	78
3,7	1.370	0.200	23
4,6	0.761	0.010	78
5	1.918	0.200	23

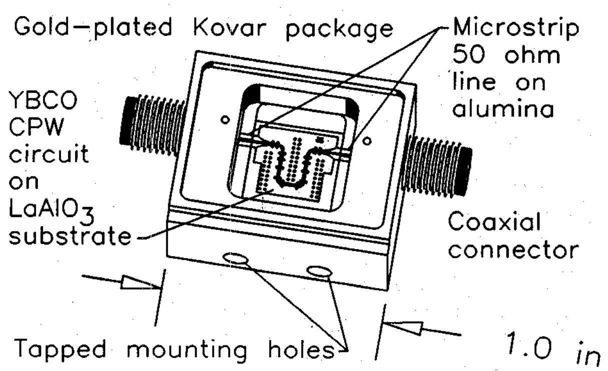

Fig. 4. Packaged filter before lid is attached.

The performance of the YBCO filters was measured in liquid nitrogen after completion of processing, patterning, soldering at 162°C in air, silver epoxy curing for 3 h at 130°C in air, wire-bonding at 130°C, 100°C bakeout in vacuum for 20 h before hermetic sealing, and electron-beam welding of the package in vacuum. Measured transmission ($|S_{21}|$) is shown in Fig. 5 for four YBCO filters, along with that for a filter made using copper, all at 77 K. For comparison, the transmission of the copper filter at 297 K is also shown. The copper filter was made with niobium–copper–gold films on both sides of an $LaAlO_3$ substrate using the deposition process described in [4] for the back-side metallization on the YBCO filter. The copper film was approximately 1 μm thick. The YBCO CPW filter responses showed lower loss in the passbands of the filters than those of the cooled copper filter (by as much as 1.7 dB at 9.5 GHz).

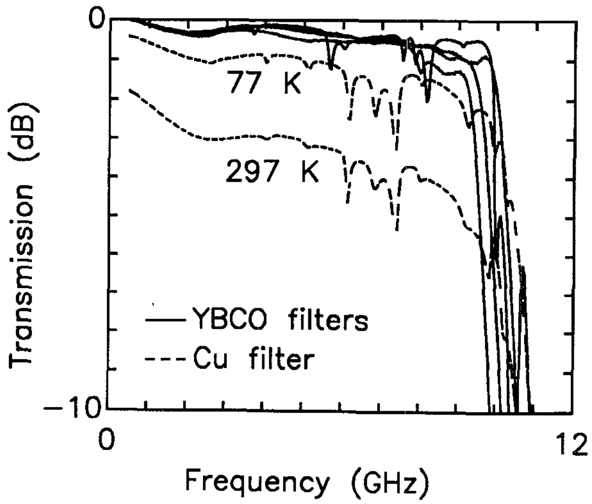

Fig. 5. Measured transmission of four YBCO filters and copper filter at 77 K, and copper filter at 297 K.

Comparisons between YBCO and copper thin films are sometimes questioned because the quality of copper thin films can vary. The analysis presented below indicates that the copper film filter used had a room-temperature conductivity of about 63% of ideal bulk copper [15], a good value for practical circuits. In any case, the estimated loss/length in the best YBCO filter, which includes any losses which may be present in addition to the conductor losses, is less throughout the passband than the conductor loss alone calculated for an ideal copper filter using these dimensions at 77 K. The superiority of YBCO over copper would be greater at lower temperatures.

The cutoff frequency of the passband varied in the superconductor filters. This was attributed to increased internal (including kinetic) inductance in the YBCO transmission lines at 77 K, which is near the critical temperature for the superconducting transition (zero-resistance T_c being 83 to 88 K in these filters after patterning). The internal inductance becomes significant as the penetration depth becomes comparable to or greater than the superconductor thickness. The penetration depth increases rapidly with increasing temperature near T_c; previous workers [13] found agreement with the Gorter–Casimir temperature dependence [16]:

$$\lambda(T) = \lambda_0 \cdot \left[1-(T/T_c)^4\right]^{-1/2} \qquad \text{for } T<T_c \qquad (8)$$

where λ is the penetration depth and λ_0 is the penetration depth at $T=0$ K. Since T_c, λ_0, and thickness vary among samples, the amount of internal inductance varies as well, causing the cutoff frequency to vary.

IV. Analysis

In this work, and in many cases involving thin-film high-T_c superconductors near T_c, the skin depths and penetration depths are comparable to the conductor thicknesses. Simple analysis assuming shallow penetration may be inadequate. In order to roughly compare the quality of the YBCO with copper and with other published results, we use the phenomenological loss equivalence method (PEM) of Lee and Itoh [17] rather than the purely empirical formulas used to model attenuation in the original design. In this model, in addition to the usual (external) impedance calculated from fields around perfect conductors, an internal impedance/length Z_t from fields penetrating into the conductor is included [17]:

$$Z_t = R_t + j\omega L_t = Z_s G \coth\left[Gwt\sqrt{j\omega\mu\sigma}\right] \qquad (9)$$

where R_t is the real part of Z_t, L_t is the internal inductance/length, ω is the radian frequency, μ is the permeability ($4\pi \times 10^{-7}$ H/m for all calculations here), σ is the complex conductivity of the conductor, coth is the hyperbolic cotangent, w is the width of the center conductor in CPW, and t is the thickness of the conductor. Z_s is the characteristic surface impedance of the conductor, defined by

$$Z_s \equiv \sqrt{j\omega\mu/\sigma} \qquad [\Omega/\text{square}] \qquad (10)$$

and G is a geometric factor, defined by

$$G = \frac{1}{\mu}\sum_m \frac{\partial L_e}{\partial n} \qquad [\text{m}^{-1}] \qquad (11)$$

where $\partial L_e/\partial n$ is the derivative of the external inductance/length L_e with respect to the incremental recession of the conductor wall m.

For an ideal transmission line with perfect conductors,

$$L_e = Z/v = (\mu/\eta_0) Z\sqrt{\epsilon_{\text{eff}}} \qquad [\text{H/m}] \qquad (12)$$

where Z is the characteristic impedance of the CPW transmission line, η_0 is the characteristic impedance of free space (377 Ω), and ϵ_{eff} is the effective relative permittivity for the CPW transmission line. Then G can be approximated by

$$G \approx \left(\frac{\sqrt{\epsilon_{\text{eff}}}}{\eta_0}\right) \cdot \frac{[Z_0(w,t,g) - Z_0(w-2\Delta, t-2\Delta, g+2\Delta)]}{\Delta} \qquad (13)$$

where g is the width of the gaps in the CPW line, and Δ is an incremental distance with $\Delta \ll w, t$. $Z_0(w,t,g)$ is the "external" impedance, which is the usual impedance calculated for CPW, but includes the effect of a thick perfect conductor. $Z_0(w,t,g)$ was obtained using formulas given by Gupta *et al.* [18], which have been tested for use in the PEM formula by Kong *et al.* [19]. The same analysis can be used if better formulas for conductor thickness effects on impedance become available.

Once R_t and $j\omega L_t$ in (9) are found, the general transmission line model (Fig. 3) can be used with

$$R = R_t \quad \text{and} \quad L = L_e + L_t \qquad (14)$$

(C is assumed the same as the usual "external" value) giving the usual transmission line result [14]:

$$\alpha_{\mathrm{dB}} = 8.686\alpha \approx \frac{8.686 R_i}{2\sqrt{L/C}} \quad (15)$$

where α is the attenuation in nepers/length, and α_{dB} is the attenuation in dB/length. The wave-slowing factor, K, in (4), which also increases the impedance in (5), is

$$K = \sqrt{1 + (L_i/L_e)}. \quad (16)$$

Using (9) to get (15) and (16) produced values for the attenuation and changes in wave velocity and impedance in the transmission line sections of the CAD model for the YBCO and copper filters.

The filter circuit models were fit to the data with only σ_{Cu} and the real and imaginary parts of σ_{YBCO} being freely adjustable parameters. The normal-metal conductivity, σ_{Cu}, was assumed to be a constant with respect to frequency, while the superconductor conductivity was assumed to have the form

$$\sigma_{\mathrm{YBCO}} = \sigma_1 + j\sigma_0 f_0/f \quad (17)$$

where σ_1 and σ_0 are constants with respect to frequency, and f_0 is a reference frequency. The conductivity in the usual two-fluid model for superconductors has the same frequency dependence and is commonly used when analyzing YBCO films [16]:

$$\sigma_{\mathrm{super}} = \sigma_n (T/T_c)^4 - j\left[1 - (T/T_c)^4\right] / (\omega\mu\lambda_0^2) \quad \text{for } T < T_c \quad (18)$$

where σ_n is the normal conductivity, T is the absolute temperature, and λ_0 is the zero-temperature penetration depth. The frequency dependence could be different when the grain boundary impedance has a significant effect. [20]. If the grain boundary impedance alone dominates, it can also be modeled as a parallel inductivity and resistivity, with the form of (17). The data on these filters probably do not provide a sufficient test of the precise frequency dependence to choose among possible forms, so the simple form of (17) was used without attempting to use (18) to relate the estimated conductivity values to intrinsic material parameters. An example of the fit (using Touchstone) between the fitted model using PEM expressions and a YBCO filter is shown in Fig. 6. The designed response (using the previous empirical model before the filter was made) is also shown; its similarity to the measured response shows that even approximate models can be adequate for practical designs.

Fitting the PEM-based model to the data for the copper filter by adjusting the value for σ_{Cu} produced the estimates

$$\sigma_{\mathrm{Cu}} \approx 3.6 \times 10^7 \ \Omega^{-1}\ \mathrm{m}^{-1} \text{ at } 297\ \mathrm{K}$$

$$\sigma_{\mathrm{Cu}} \approx 1.2 \times 10^8 \ \Omega^{-1}\ \mathrm{m}^{-1} \text{ at } 77\ \mathrm{K}.$$

Fitting the PEM-based model to the data for the best-packaged YBCO filter by adjusting the values for σ_1 and

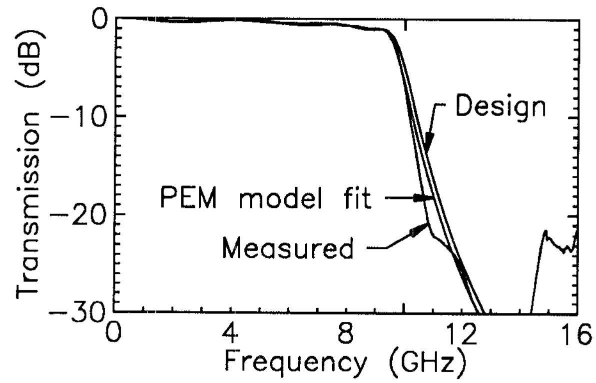

(a)

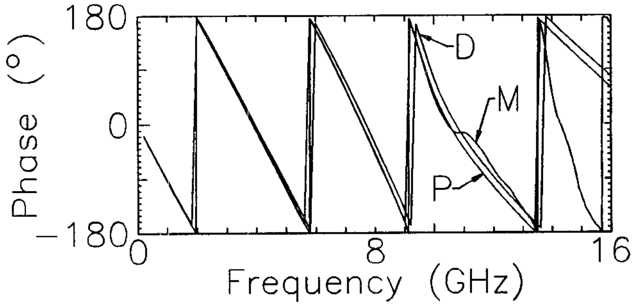

(b)

Fig. 6. Comparison of design using empirical model, measured YBCO filter transmission, and fit to measurement using PEM-based model. (a) $|S_{21}|$ in dB. (b) Phase of S_{21}. D denotes design, M measured response, and P fit to measurement using PEM-based model.

σ_0 in (17) produced the estimate

$$\sigma_{\mathrm{YBCO}} \approx 5.6 \times 10^6 - j6.2 \times 10^7 (f_0/f)\ \Omega^{-1}\ \mathrm{m}^{-1} \text{ at } 77\ \mathrm{K}$$

where $f_0 = 9$ GHz. The characteristic surface impedance defined by (10) then gives

$$Z_{s,\mathrm{Cu}} \approx 0.031 + j0.031\ \Omega \text{ at } 9\ \mathrm{GHz at } 297\ \mathrm{K}$$

$$Z_{s,\mathrm{Cu}} \approx 0.017 + j0.017\ \Omega \text{ at } 9\ \mathrm{GHz at } 77\ \mathrm{K}$$

$$Z_{s,\mathrm{YBCO}} \approx 0.002 + j0.034\ \Omega \text{ at } 9\ \mathrm{GHz and at } 77\ \mathrm{K}.$$

Because (10) would give measured impedance/square values only when the penetration or skin depth is much less than the film thicknesses and when the anomalous skin effect is negligible [15], Z_s given by (10) represents a figure of merit rather than what may be measured in a thin film. This allows a rough comparison with other published surface resistance values. For example, ideal room-temperature cooper with $\sigma = 5.8 \times 10^7\ \Omega^{-1}\mathrm{m}^{-1}$ has surface impedance $Z_s \approx 0.025 + j0.025\ \Omega$ at 9 GHz. The quality factor formula [11]

$$Q = \pi/(\alpha\lambda_g) = (8.686\pi)/(\alpha_{\mathrm{dB}}\lambda_g) \quad (19)$$

where λ_g is the wavelength in the transmission line, gives the estimated values (Table II) for the best-packaged YBCO filter.

The values for σ and Z_s found by the analysis above are an average over the area of the CPW lines and are approximate. The actual conductivity probably varies for different sections of CPW, both because different line widths are likely to have different amounts of degradation caused by processing and because the deposited film

TABLE II
ESTIMATED ATTENUATION COEFFICIENTS AND Q VALUES

Width of Center Conductor of CPW	α_{dB} [dB/m] 9 GHz, 77K		Q 9 GHz, 77K	
	Cu	YBCO	Cu	YBCO
5–6 μm	90	20	30	100
46 μm	30	6	90	500
196 μm	50	5	60	600

properties may not be uniform over the entire area. Also, other possible sources of loss have not been included, such as loss in input and output imperfections and bond wires. Dielectric losses are expected to be small for loss tangents of 0.0001 or smaller using the usual formulas for CPW and microstrip [18] and were not included. Thus, the estimates found above for the YBCO may be conservative.

The PEM formulas can be used for design as well as analysis, with the advantages of fewer adjustable parameters which must be determined than the empirical formulas used for the original filter design; only the complex conductivity is adjustable.

V. Conclusion

The design of coplanar waveguide filters using $YBa_2Cu_3O_{7-\delta}$ on $LaAlO_3$ has been described. Complete packaged CPW filters of YBCO using transmission lines having dimensions expected to be useful in integrated circuits have been made which exhibit losses superior to those of a corresponding copper filter throughout the 0 to 9.5 GHz passband. The PEM model of Lee and Itoh [17] for films of thickness comparable to the skin depth or penetration depth can be used with commercial microwave CAD software and was employed here to compare the surface impedances of the YBCO and copper filters. The models, while using approximate formulas, can be used for design. As more extensive data, verified closed-form formulas for CPW, and improved films become available, CPW components of YBCO should become standard elements in design and use.

Acknowledgment

The authors wish to express their thanks to J. Bautista for advice and for providing Advanced CryoElectronics laboratory facilities; to J. Bowen, D. Neff, G. Ortiz, and L. Duffy for advice; and to S. Chavez, C. Cruzan, and J. Rice for assembly and wire-bonding expertise. D. Antsos, working toward more accurate calculations, gave constructive criticism.

References

[1] C. P. Wen, "Coplanar waveguide: A surface strip transmission line suitable for nonreciprocal gyromagnetic device applications," *IEEE Trans. Microwave Theory Tech.*, vol. MTT-17, pp. 1087–1090, Dec. 1969.

[2] A. A. Valenzuela and P. Russer, "High Q coplanar transmission line resonator of $YBa_2Cu_3O_{7-x}$ on MgO," *Appl. Phys. Lett.*, vol. 55, pp. 1029–1031, 4 Sept 1989.

[3] A. A. Valenzuela, B. Daalmans, and B. Roas, "High-Q coplanar transmission line resonator of $YBa_2Cu_3O_{7-x}$ on $LaAlO_3$," *Electron. Lett.*, vol. 25, pp. 1435–1436, 12 Oct. 1989.

[4] W. Chew *et al.*, "High T_c superconductor coplanar waveguide filter," submitted to *IEEE Electron Device Lett.*, 1991.

[5] R. W. Simon *et al.*, "Low-loss substrate for epitaxial growth of high-temperature superconductor thin films," *Appl. Phys. Lett.*, vol. 53, pp. 2677–2679, 26 Dec. 1988.

[6] M. C. Nuss *et al.*, "Propagation of terahertz bandwidth electrical pulses on $YBa_2Cu_3O_{7-\delta}$ transmission lines on lanthanum aluminate," *Appl. Phys. Lett.*, vol. 54, pp. 2265–2267, 29 May 1989.

[7] F. A. Miranda, W. L. Gordon, V. O. Heinen, B. T. Ebihara, and K. B. Bhasin, "Measurements of complex permittivity of microwave substrates in the 20 to 300 K temperature range from 26.5 to 40.0 GHz," presented at 1989 Cryogenic Engineering Conf., University of California, Los Angeles, Los Angeles, CA, July 24–28, 1989; printed as NASA Technical Memorandum 102123.

[8] Hewlett-Packard Product Note 8510-6, "On wafer measurements using the HP8510 Network Analyzer and Cascade Microtech wafer probes," Hewlett-Packard, Palo Alto, CA, 1986.

[9] G. Ghione and C. Naldi, "Parameters of coplanar waveguides with lower ground planes," *Electron. Lett.*, vol. 19, pp. 734–735, 1983.

[10] G. Hasnain, A. Dienes, and J. R. Whinnery, "Dispersion of picosecond pulses in coplanar transmission lines," *IEEE Trans. Microwave Theory Tech.*, vol. MTT-34, pp. 738–741, June 1986.

[11] T. C. Edwards, *Foundations for Microstrip Circuit Design*. New York: Wiley, 1981.

[12] Hewlett-Packard Product Note 8510-8, "Applying the HP8510B TRL calibration for non-coaxial measurements," Hewlett-Packard Co., Palo Alto, CA, 1987.

[13] K. B. Bhasin *et al.*, "Performance and modeling of superconducting ring resonators at millimeter-wave frequencies," in *1990 IEEE MTT-S Int. Microwave Symp. Dig.*, May 1990, pp. 269–272.

[14] S. Ramo, J. R. Whinnery, and T. Van Duzer, *Fields and Waves in Communication Electronics*. New York: Wiley, 1965.

[15] L. W. Duncan, "Computation of RF surface resistance using the anomalous skin effect theory," *IEEE Trans. Microwave Theory Tech.*, vol. MTT-10, pp. 130–131, Feb. 1968.

[16] T. Van Duzer and C. W. Turner, *Principles of Superconductive Devices and Circuits*. New York: Elsevier, 1981.

[17] H. Y. Lee and T. Itoh, "Phenomenological loss equivalence method for planar quasi-TEM transmission lines with a thin normal conductor or superconductor," *IEEE Trans. Microwave Theory Tech.*, vol. 37, pp. 1904–1909, Dec. 1989.

[18] K. C. Gupta, R. Garg, and I. J. Bahl, *Microstrip Lines and Slotlines*. Norwood, MA: Artech House, 1979, ch. 7.

[19] K.-S. Kong, C. W. Kuo, T. Kitazawa, and T. Itoh, "Analysis of the superconducting coplanar waveguide by combining spectral domain method and phenomenological equivalence method," *Electron. Lett.*, vol. 26, pp. 1558–1560, 13 Sept. 1990.

[20] T. L. Hylton *et al.*, "Weakly coupled grain model of high frequency losses in high T_c superconducting thin films," *Appl. Phys. Lett.*, vol. 53, pp. 1343–1345, 3 Oct. 1988.

Wilbert Chew received the Ph.D. degree from UCLA, in 1988, where he developed a millimeter-wave integrated quasi-optical FET mixer and imaging and ranging demonstrations with a small array of such mixers.

From 1981 to 1983, he was a Member of the Technical Staff at the Hughes Aircraft Company doing modeling and systems analysis of infrared imaging systems. In 1989, he joined the Jet Propulsion Laboratory, California Institute of Technology, where he has participated in antenna array analysis and the development of microwave applications for high-temperature superconductors.

A. Landis Riley (M'82) obtained the Ph.D. degree in electrical engineering in 1971 from Johns Hopkins University.

He is manager of NASA Communications Technology Programs at the Jet Propulsion Laboratory. He has more than 20 years of experience in the design and development of microwave and millimeter-wave com-

ponents, subsystems, and instruments. His experience includes four years at the Westinghouse Electric Corporation designing active microwave components, four years at MIT Lincoln Laboratory developing spaceborne frequency synthesizer microwave subsystems, and 12 years at JPL involved in component and subsystem design at frequencies as high as 230 GHz. This work has included development of a 55 GHz spaceborne mixer, system development of the Microwave Limb Sounder instrument, and development of 115 GHz and 230 GHz radiometer systems for remote sensing for the Martian atmosphere. He has been responsible for the design and development of microwave and millimeter-wave solid-state power amplifier systems. He also managed the development of the JPL device for the Naval Research Laboratory HTSSE program.

Daniel L. Rascoe (M'84) received the Ph.D. degree in physics in 1978 from the University of Illinois, where his research involved state-of-the-art low-temperature refrigeration, millimeter-wave (70–90 GHz) electron spin resonance, and phonon transport through superfluid helium.

He has more than 11 years of experience in the research, development, and production of microwave hardware and subsystems for spacecraft. This includes eight years at Hughes Aircraft Space and Communications Group, where he designed and developed communications receivers, low-noise amplifiers, and solid-state power amplifiers at operating frequencies from 2 to 20 GHz. For the past four years, he has been a Member of the Technical Staff at JPL in the Spacecraft RF Development Group of the Spacecraft Telecommunications Equipment Section. At JPL, he has been the cognizant engineer for the design of a Ka-band (32 GHz) electronically steered planar array utilizing microwave monolithic integrated circuits and a member of the team that fabricated and delivered HTS microwave filters to the Navy's High Temperature Superconducting Space Experiment (HTSSE).

Brian D. Hunt received the Ph.D. degree in applied physics from Cornell University in 1984. His thesis research involved a study of three-terminal superconducting devices and nonequilibrium superconductivity utilizing a novel double edge junction structure fabricated by electron beam lithography.

He worked for three years at the General Electric Corporate Research and Development Laboratory, where he investigated the application of Si molecular beam epitaxy to the growth of epitaxial silicide/Si heterostructures and devices including a $Si/CoSi_2/Si$ metal base transistor. He is currently a member of the technical staff in the Microdevices Laboratory at the Jet Propulsion Laboratory, California Institute of Technology. Since arriving at JPL, in 1987, he has initiated the high-temperature superconductor thin-film devices program. His work at JPL has focused on epitaxial growth studies of YBaCuO by laser ablation, as well as on high-T_c device studies utilizing superconductor/normal-metal/superconductor (SNS) structures to optimize the surface electrical properties of YBaCuO. He invented and fabricated a novel edge-geometry YBaCuO/Au/Nb device structure, as well as the first NbN/MgO/NbN edge-geometry tunnel junctions. He collaborated on a successful project to fabricate and deliver YBaCuO microwave filters for a satellite launch.

Marc C. Foote received the Ph.D. degree in low-temperature physics from the University of Illinois, Urbana-Champaign. The work for his thesis involved electrical properties of disordered materials and was performed at AT&T Bell Laboratories under a Ph.D. scholarship program.

He is currently a member of the technical staff in the Microdevices Laboratory at the Jet Propulsion Laboratory, California Institute of Technology. His current work involves developing YBaCuO thin-film growth techniques as well as fabricating superconductor/normal-metal/superconductor devices using this material.

Thomas W. Cooley joined the Jet Propulsion Laboratory, California Institute of Technology, in 1988, after receiving the B.S. degree from Rensselaer Polytechnic Institute. He has worked on microwave phased array antenna design and integration. He received the M.S. degree from Caltech in June 1991.

Louis J. Bajuk received the B.A. degree in physics in 1989 from Oberlin College, where he helped initiate a high-temperature superconductor research program.

He is currently a member of the Nanodevices and Superconductivity Group of the Microdevices Laboratory at the Jet Propulsion Laboratory, California Institute of Technology, where he has worked on the deposition of laser-ablated high-temperature superconductor thin films, as well as on the fabrication of YBCO thin-film passive microwave devices.